PAPER

Invisible metal-grid transparent electrode prepared by electrohydrodynamic (EHD) jet printing

IOP PUBLISHING JOURNAL OF PHYSICS D: APPLIED PHYSICS

J. Phys. D: Appl. Phys. **46** (2013) 155103 (5pp) doi:10.1088/0022-3727/46/15/155103

Invisible metal-grid transparent electrode prepared by electrohydrodynamic (EHD) jet printing

Yonghee Jang[1], **Jihoon Kim**[2,3] **and Doyoung Byun**[1,3]

[1] School of Mechanical Engineering, SungKyunKwan University, Suwon, Gyeonggi-do 440-746, Korea
[2] Division of Advanced Materials Engineering, Kongju National University, Cheonan, Chungchungnam-do 331-717, Korea

E-mail: Jihoon.kim@kongju.ac.kr (J Kim) and dybyun@skku.edu (D Byun)

Received 15 November 2012, in final form 14 February 2013
Published 18 March 2013
Online at stacks.iop.org/JPhysD/46/155103

Abstract

Invisible Ag-grid transparent electrodes (TEs) were prepared by electrohydrodynamic (EHD) jet printing using Ag nano-particle inks. Ag-grid width less than 10 μm was achieved by the EHD jet printing, which was invisible to the naked eye. The Ag-grid line-to-line distance (pitch) was modulated in order to investigate the electrical and optical properties of the EHD jet-printed Ag-grid TEs. The decrease in the sheet resistance at the expense of the transmittance was observed as the Ag-grid pitch decreased. The figure of merit of Ag-grid TEs with various Ag-grid pitches was investigated in order to determine the optimum pitch condition for both electrical and optical properties. With the 150 μm Ag-grid pitch, the EHD jet-printed Ag-grid TE has the sheet resistance of 4.87 $\Omega\,\mathrm{sq}^{-1}$ and the transmittance of 81.75% after annealing at 200 °C under near-infrared. Ag filling factor (FF) was defined to predict the electrical and optical properties of Ag-grid TEs. It was found that the measured electrical and optical properties were well simulated by the theoretical equations incorporating FF. The EHD jet-printed invisible Ag-grid TE with good electrical and optical properties implies its promising application to the printed optoelectronic devices.

(Some figures may appear in colour only in the online journal)

1. Introduction

Printing technology currently attracts significant attention from many different fields of microelectronics such as flexible displays, solar cells, touch panels, light-emitting diodes, thin-film transistor, memory devices, sensors, biological devices and passive circuit elements [1–12]. Such a versatile application of the printing technology results from its ability to directly deposit various functional materials on a substrate in a desired pattern with more efficient material utilization compared with the conventional vacuum-based process [13–17].

Among the various printing techniques, electrohydrodynamic (EHD) jet printing has recently gained a lot of interest because of its potential for high-resolution printing. A strong electric field applied to the nozzle leads to the elongation of the ink on the tip of the nozzle and the breakout of the ink into droplets whose size is smaller than the diameter of the nozzle [18, 19]. This unique capability of EHD jet printing results in an easy realization of fine patterning with a high resolution.

Transparent electrode (TE) is one of the most critical materials for various optoelectronic devices and components. Most TEs are synthesized based on the metal oxides including appropriate doping elements, most commonly tin-doped indium oxide (ITO). However, the oxide-based TEs, currently, are assessed as an unfavourable choice of materials for future optoelectronic applications due to the brittleness of oxide-based TEs, the high temperature treatment involved in their fabrication, and their multicomponent structure incompatible with some active materials in devices [20–23]. In addition, the fabrication of oxide-based TEs employs an expensive vacuum-based process which prevents the cost reduction for

[3] Authors to whom any correspondence should be addressed.

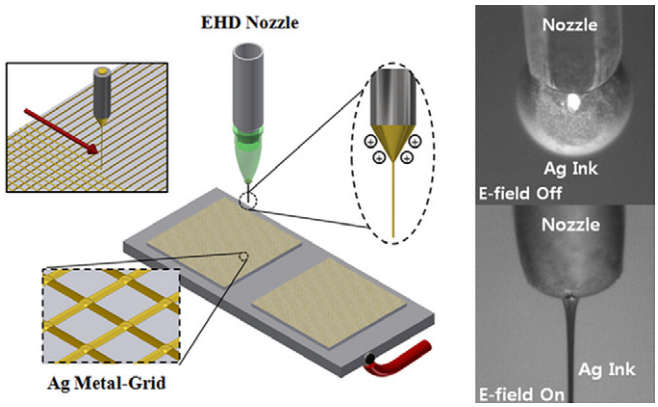

Figure 1. Schematic diagram of the EHD jet printing process for Ag-grid TEs. The ink ejection images from the nozzle without and with the electrical field are presented on the right side.

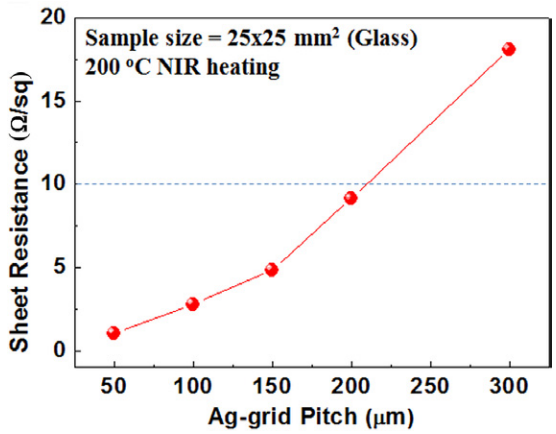

Figure 2. Electrical properties (sheet resistance) of EHD jet-printed Ag-grid TEs. The line pitch in the Ag grid varies from 50 to 300 μm.

future optoelectronic devices. These drawbacks associated with oxide-based TEs have led to many attempts to replace them with alternative materials such as carbon nanotubes, graphene films, metal nanowires and metal-grid electrodes [24]. Among those alternatives, metal-grid electrodes become very promising if considered with the assistance of printing technology in terms of its product cost, since printing technology helps improve the efficiency of material utilization as well as simplifying the process steps for the fabrication of metal-grid TEs. There are several reports on the realization of metal-grid TEs. However, most of their fabrication methods were restricted to imprinting and metal lithography which involve rather complicated fabrication steps [25–27].

In this work, we employed EHD jet printing which is one of the non-contact printing techniques. The line width of the metal-grid TE patterned by EHD jet printing was less than 10 μm, which is beyond the pattern resolution capability of the human eye [28, 29]. The optical and electrical properties of the EHD jet-printed invisible metal-grid TEs were investigated by adjusting the line-to-line spacing (pitch) in the metal-grid TEs and also compared with the theoretical prediction based on the geometry of the metal-grid.

2. Experimental procedure

EHD jet printing unit (NP-200, ENJET) was used in the experiment. A schematic diagram of the EHD printing process for Ag-grid TEs is presented in figure 1. A stainless-steel nozzle whose inner diameter is 100 μm is equipped on the head of the unit. The voltage of 2 kV was induced over the distance of 5 mm between the nozzle and substrate. The flow rate in the syringe pump is maintained at 150 nl min^{-1}. the pattern speed is fixed at 30 cm s^{-1}. A commercial Ag ink (ENJET) designed for the EHD jet printing was used in the fabrication of the metal-grid TEs. The solvent used in the formulation of the Ag ink was triethylene glycol monoethyl ether (Sigma-Aldrich). The surface tension, density and viscosity of the Ag ink are 52.1 dyne cm^{-1}, 3.35 g cm^{-3} and 4300 cPs, respectively. The solid content of Ag nano-particles in the ink was 70 wt%. The Ag ink went through a stirring process by homogenizer and vortex mixer before printing. Since relatively high viscosity ink (4300 cPs) was used in this work, a continuous con-jet line (not pulsating droplets) from the nozzle was extracted by the applied electric field as shown in the right part of figure 1. EHD jet-printed Ag-grid TEs with the dimension of 20 × 20 mm^2 were prepared on the glass substrate (25 × 25 mm^2). The EHD jet-printed Ag-grid TEs were annealed in air atmosphere under near-infrared (NIR) irradiation at 200 °C for 30 min. The width and thickness of the EHD jet-printed Ag-grid pattern were measured by field emission scanning electron microscope (FE-SEM; Nova 200). The electrical properties of the EHD jet-printed Ag-grid TEs such as sheet resistance were measured by Hall measurement (ECOPIA HMS3000). Optical transmittance measurements were implemented using a UV/visible spectrometer (JASCO V-570) in the wavelength ranging from 300 to 800 nm.

3. Results and discussion

Figure 2 shows the sheet resistance of EHD jet-printed Ag-grid TEs on glass substrates as a function of Ag line-to-line pitch after NIR heating at 200 °C. It was observed that the sheet resistance of Ag-grid electrodes gradually decreased with decreasing Ag-grid line pitch from 300 to 50 μm. The sheet resistances at the pitches less than 200 μm were less than 10 Ω sq^{-1}, which were better than the conventional sputtered ITO films [30]. However, since the smaller Ag-grid pitch means more Ag-grid lines employed in the electrode, the transmittance of the Ag-grid electrode in the visible region is expected to be degraded due to the scattering and reflection of the incident light on the Ag-grid pattern. In order to investigate this unfavourable decline in the transmittance, the optical transmittance spectra of the EHD jet-printed Ag-grid electrodes with various Ag-grid pitches were measured. Figure 3 presents the optical transmittance at a wavelength of 550 nm for the EHD jet-printed Ag-grid TEs. The inset of figure 3 shows the transmittance over the wavelength from 300 to 800 nm. The transmittance decreased from 86.7% to 67.0% with decreasing the Ag-grid pitch from 300 to 50 μm. However, transmittance higher than 80% was sustained at the pitches above 150 μm. For information, the bare glass substrate had a transmittance of 91% at 550 nm.

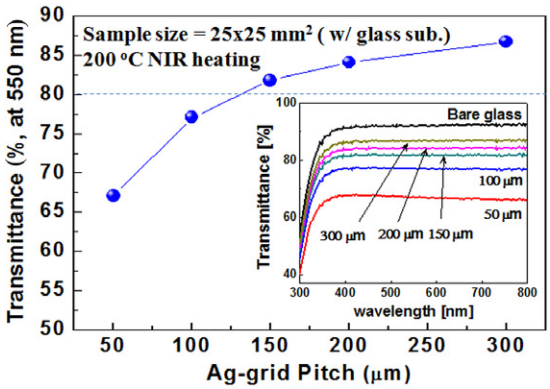

Figure 3. Optical transmittance of EHD jet-printed Ag-grid TEs measured at 550 nm as a function of the grid line pitch in Ag-grid TEs. The inset presents optical transmittance spectra over a visible wavelength range. All transmittance data were measured from the samples including both Ag-grid TE at a given pitch and the glass substrate.

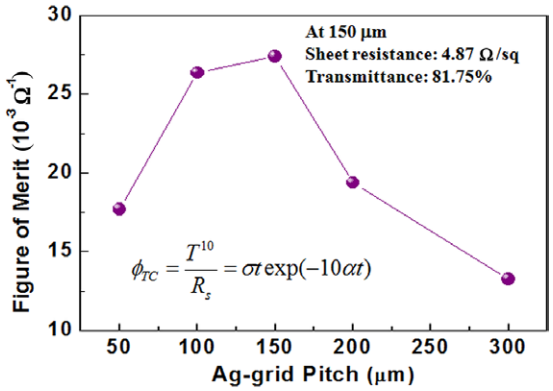

Figure 4. Figure-of-merit values for the EHD jet-printed Ag-grid TEs as a function of Ag-grid pitch.

It was evident from figures 3 and 4 that the electrical property of the EHD jet-printed Ag-grid TE was enhanced at the expense of its optical property, the concept of the figure of merit (ϕ_{FM}) defined by Haccke [31] was used to determine the optimum Ag-grid pitch which led to the best trade-off between sheet resistance and transmittance:

$$\phi_{FM} = \frac{T^{10}}{R_{sheet}} = \sigma t \exp(-10\alpha t), \tag{1}$$

where T is the transmittance at a wavelength of 550 nm, R_{sheet} is the sheet resistance (Ω sq^{-1}), σ is the electrical conductivity (Ω^{-1} cm^{-1}), t is the film thickness (cm), and α is the optical absorption coefficient (cm^{-1}). Figure 4 presents ϕ_{FM} values of the EHD jet-printed Ag-grid TE as a function of Ag-grid pitch. It indicates that ϕ_{FM} increases with increasing Ag-grid pitch up to 150 μm since the increase in the transmittance is more substantial compared with the increase in the sheet resistance of the TE. However, the further increase in the Ag-grid pitch results in the decrease in ϕ_{FM}, indicating that the optimum pitch of the Ag grid is 150 μm for the EHD jet-printed Ag-grid TEs.

The electrical and optical properties of the EHD jet-printed Ag-grid TE are dependent upon the amount of Ag-grid lines on the substrate which can be defined by a filling factor (FF)

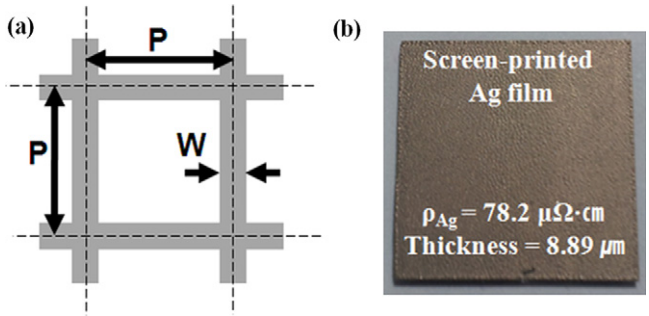

Figure 5. (*a*) Geometry of the Ag-grid pattern leading to the definition of Ag filling factor. (*b*) The resistivity of the ink was obtained from the screen-printed Ag films with the same Ag ink used in the EHD jet printing. The optical microscopic image of the film is presented.

of Ag-grid with the following equation:

$$\mathrm{FF} = \frac{(p \times w) + [(p - w) \times w]}{p^2}, \tag{2}$$

where p and w are the Ag-grid pitch and the width of the Ag-grid line, respectively, as described in figure 5(*a*). From the calculated value of FF, it is possible to predict both the sheet resistance ($R_{s,\mathrm{Ag\ grid}}$) and the transmittance ($t_{\mathrm{Ag\ grid}}$) of the EHD jet-printed Ag-grid TE by the following equations:

$$R_{s,\mathrm{Ag\ grid}} = \xi \frac{\rho_{\mathrm{Ag\ grid}}}{t_{\mathrm{Ag\ grid}}} \frac{1}{\mathrm{FF}}, \tag{3}$$

$$T_{\mathrm{Ag\ grid}} = T_{\mathrm{Bare}} \times (1 - \mathrm{FF}), \tag{4}$$

where $\rho_{\mathrm{Ag\ grid}}$ is the resistivity of the Ag ink used to form the Ag grid by EHD jet in this experiment, $t_{\mathrm{Ag\ grid}}$ is the thickness of the Ag-grid line, ξ is a correction factor [32], T_{Bare} is the transmittance of the bare glass substrate. The correction factor (ξ) depends on a given printing process and can be obtained by fitting the experiment data. A similar approach for the prediction of metal-grid TEs was carried out by Ghosh *et al* [32], except that a different definition of Ag FF was used in our analysis. In our calculation, $\rho_{\mathrm{Ag\ grid}}$ was obtained from the screen-printed Ag films with the same Ag ink used in this experiment. The Ag film showed the resistivity of 78.2 $\mu\Omega$ cm with its thickness of 8.9 μm after the NIR heat treatment at 200 °C for 30 min (figure 5(*b*)). Figure 6 shows the comparison between the predicted and measured values of the sheet resistance and transmittance for the EHD jet-printed Ag-grid TEs as a function of Ag-grid pitch. The experimentally measured data for the sheet resistance and transmittance of the EHD jet-printed Ag-grind TEs well follow the trend of the predicted values with a minimal deviation. We believe this deviation arises from the variation in the width and height of the printed lines, which is somehow inevitable in the liquid-based printing technology.

Figure 7 shows the FE-SEM and optical images of the EHD jet-printed Ag-grid TE. The above-mentioned small variation in the dimension of the printed lines was observed in figure 7(*a*). The cross-sectional image in figure 7(*b*) indicates that the width and height of the EHD jet-printed Ag grid are 7.5 μm and 1.46 μm, respectively. Figure 7(*c*)

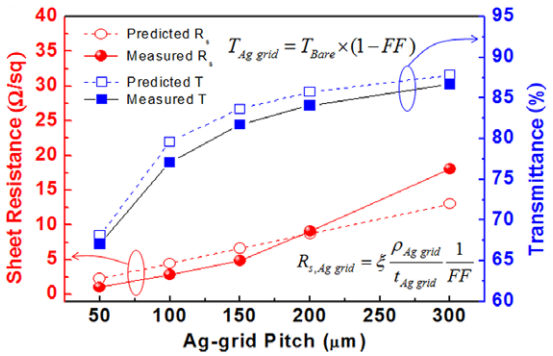

Figure 6. Theoretical prediction of the sheet resistance and transmittance for EHD jet-printed Ag-grid TE with comparison to the experimentally observed values.

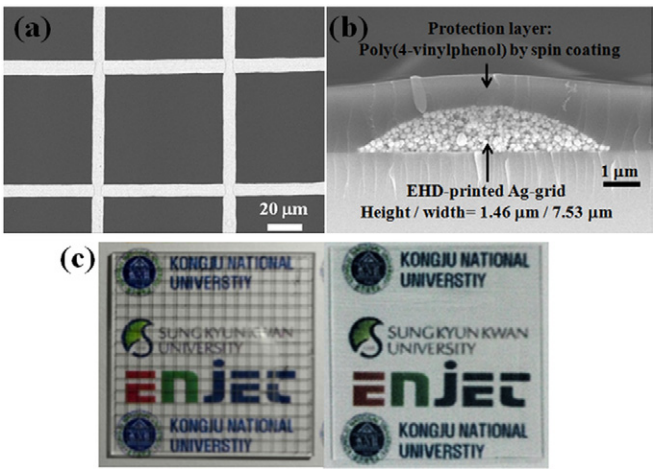

Figure 7. (*a*) FE-SEM planar and (*b*) cross-sectional image of EHD jet-printed Ag-grid TEs. (*c*) Optical microscopic images of Ag-grid TEs printed by both inkjet and EHD jet printing. Ag grid patterned by EHD jet printing is not visible to the naked eye.

compares the EHD jet-printed Ag-grid TE to an Ag-grid TE prepared by the conventional inkjet printing method. The inkjet-printed Ag-grid TE was fabricated by UJ200 inkjet-printing unit (Unijet) which is equipped with a nozzle (30 pl) from SMJET (Samsung) [33]. The width of the inkjet-printed Ag grid was 50 μm, which is visible to the naked eye. Even if the commercially available smallest nozzle (1 pl) is employed, it is known that its achievable line resolution is limited to 20–30 μm [34] which is still detectable by the naked eye [28, 29]. However, the Ag grid patterned by EHD jet is invisible, as shown in figure 7(*c*), since its line width (about 7 μm) is beyond the human eye's resolution. It indicates that EHD jet printing is a promising method to fabricate an invisible fine patterned metal-grid TE with good electrical and optical properties, which can be widely applied to optoelectronic devices without any cosmetic issues due to the appearance of metal pattern.

4. Conclusions

In this paper, the EHD jet printing of invisible Ag-grid TEs was investigated. The employment of EHD jet printing enabled us to realize the printed line width of the Ag-grid TE less than 10 μm, which is invisible to the naked eye. The Ag-grid line-to-line pitch was adjusted in order to define an optimum condition on the trade-off between electrical and optical properties of Ag-grid TEs since the reduction in pitch resulted in the improvement of the electrical property at the expense of the optical property. With 150 μm Ag-grid pitch, the EHD jet-printed Ag-grid TE has a sheet resistance of 4.87 $\Omega\,\mathrm{sq}^{-1}$ and transmittance of 81.75% after annealing at 200 °C under near-infrared (NIR). A theoretical prediction of both electrical and optical properties of Ag-grid TEs was made based on Ag filling factor which is correlated with the geometry of Ag-grid TEs. The predicted values for the sheet resistance and transmittance of EHD jet-printed Ag-grid TEs were well matched with the experimental observation. The good electrical and optical properties of the invisible Ag-grid TEs indicate their promising application to printed optoelectronic devices.

Acknowledgments

This research was supported by the Agency for Defense Development in Korea under the Contract No UE115092GD. This work was also supported by the Basic Science Research Program through the National Research Foundation of Korea (NRF) funded by the Ministry of Education, Science and Technology (2012R1A1A1039752 and 2011-0016461) and by the Industrial Core Technology Development Project through the Ministry of Knowledge and Commerce (10035644-2012-03).

References

[1] Jaworek A 2007 *J. Mater. Sci.* **42** 266
[2] Chiarot P R, Sullivan P and Mrad R B 2011 *J. Microelectromech. Syst.* **20** 1241
[3] Singh M, Haverinen H M, Dhagat P and Jabbour G E 2010 *Adv. Mater.* **22** 673
[4] Haverinen H M, Myllylä R A and Jabbour G E 2009 *Appl. Phys. Lett.* **94** 073108
[5] Haverinen H M, Myllyä R A and Jabbour G E 2010 *J. Disp. Technol.* **6** 87
[6] Gans B D, Hoeppener S and Schubert U S 2006 *Adv. Mater.* **18** 910
[7] Mager D, Peter A, Tin L D, Fischer E, Smith P J, Hennig J and Korvink J G 2010 *IEEE Trans. Med. Imaging* **29** 482
[8] Oh Y, Lee S, Kim H and Kim J 2012 *J. Electrochem. Soc.* **159** H777
[9] Lim J, Kim J, Yoon Y J, Kim H, Yoon H G, Lee S and Kim J 2012 *Curr. Appl. Phys.* **12** e14
[10] Lim J, Cho D, Eun K, Choa S, Na S, Kim J and Kim H 2012 *Sol. Energy Mater. Sol. Cells* **105** 69
[11] Kim J, Na S and Kim H 2012 *Sol. Energy Mater. Sol. Cells* **98** 424
[12] Oh Y, Yoon H G, Lee S, Kim H and Kim J 2012 *J. Electrochem. Soc.* **159** B35
[13] Sirringhaus H, Kawase T, Friend R H, Shimoda T, Inbasekaran M, Wu W and Woo E P 2000 *Science* **290** 2123
[14] Stree R A, Wong W S, Ready S E, Chabinyc M L, Arias A C, Limb S, Salleo A and Lujan R 2006 *Mater. Today* **9** 32
[15] Kawase T, Sirringhaus H, Friend R H and Shimoda T 2001 *Adv. Mater.* **13** 1601
[16] Bharathan J and Yang Y 1998 *Appl. Phys. Lett.* **72** 2660

[17] Hebner T R, Wu C C, Marcy D, Lu M H and Sturm J C 1998 *Appl. Phys. Lett.* **72** 519
[18] Nguyen V D, Schrlau M G, Tran S B, Bau H H, Ko H S and Byun D 2009 *J. Nanosci. Nanotechnol.* **9** 7298
[19] Nguyen V D and Byun D 2009 *Appl. Phys. Lett.* **94** 173509
[20] O'Connor B, Haughn C, An K H, Pipe K P and Shtein M 2008 *Appl. Phys. Lett.* **93** 223304
[21] Wang Y, Chen X, Zhong Y, Zhu F and Loh K P 2009 *Appl. Phys. Lett.* **95** 063302
[22] Ghosh D S, Martinez L, Giurgola S, Vergani P and Pruneri V 2009 *Opt. Lett.* **34** 325
[23] Krautz D, Cheylan S, Ghosh D S and Pruneri V 2009 *Nanotechnology* **20** 275204
[24] Hecht D S, Hu L and Lrvin G 2011 *Adv. Mater.* **23** 482
[25] Kang M, Kim M, Kim J and Guo L J 2008 *Adv. Mater.* **20** 4408
[26] Zou J, Yip H, Hau S K and Jen A K-Y 2010 *Appl. Phys. Lett.* **96** 203301
[27] Galagan Y, Rubingh J J M, Andriessen R, Fan C, Blom P W M, Veenstra S C and Kroon J M 2011 *Sol. Energy Mater. Sol. Cells* **95** 1339
[28] http://sciencefocus.com/qa/how-small-can-naked-eye-see, viewed September 8 2012
[29] Blayo A and Pineaux B 2005 *Joint sOC-EUSAI Conf. (Grenoble, France)*
[30] Jeong J, Kim J and Kim H 2011 *Sol. Energy Mater. Sol. Cells* **95** 1974
[31] Haacke G 1976 *J. Appl. Phys.* **47** 4086
[32] Ghosh D S, chen T L and Pruneri V 2010 *Appl. Phys. Lett.* **96** 041109
[33] Hwang M, Jeong B, Moon J, Chun S and Kim J 2011 *Mater. Sci. Eng.* B **176** 1128
[34] Ko S H, Pan H, Grigoropoulos C P, Luscombe C K, Frechet J M J and Poulikakos D 2007 *Nanotechnology* **18** 345202